Distribution of neutrons and protons in elongated targets

Miroslav Zeman[1,2,*], *Jindrich* Adam[1], *Anton* Baldin[2], *Miriama* Brunciakova[1,2], *Sergey* Gustov[2], *Karel* Katovsky[1], *Jurabek* Khushvaktov[2], *Dusan* Kral[1], *Alexander* Solnyshkin[2], *Josef* Svoboda[1,2], *Ondrej* Stastny[1], *Pavel* Tichy[2,3,4], *Sergey* Tyutyunikov[2], *Jitka* Vrzalova[2,3], *Vladimir* Wagner[3], and *Lukas* Zavorka[2]

[1]Brno University of Technology, Faculty of Electrical Power Engineering, Brno, Czech Republic
[2]Joint Institute for Nuclear Research, Dubna, Russian Federation
[3]Nuclear Physics Institute of the ASCR, Rez, Czech Republic
[4]Czech Technical University in Prague, Department of Nuclear Reactors, Prague, Czech Republic

Abstract. Analysis of neutron distribution was carried out for two elongated targets. The targets have cylindrical shape and are made of lead and carbon, respectively. The dimensions are approximately one meter in length and 19 cm in diameter. The targets were irradiated with 660 MeV proton beam at Phasotron accelerator at the Joint Institute for Nuclear Research. The total number of protons was 2.35(18)E15 for the experiment with carbon target and the total number of particles at the second experiment was 2.32(19)E15. The produced neutron field was monitored by cobalt threshold activation detectors at various positions. The activation detectors were measured by means of gamma spectroscopy using HPGe detectors. Reaction rates of different radionuclides produced in the activation detectors were determined and the results from both experiments were compared. The ratios were calculated for 7 reactions produced in cobalt detectors. The ratio of the reaction rates shows that the number of residual nuclei with higher threshold energies is higher for experiment with carbon target than for the experiment with the lead target.

1 Introduction

Nuclear power plants generate increasing volume of Spent Nuclear Fuel (SNF) each year and reserves of fresh fuel are limited. It is possible to use the SNF in the future because it contains energy in the form of minor actinides, for example. One way is to focus on Accelerator Driven Systems (ADS). The experimental research on ADS is conducted from the beginning of 1990's, where two main projects were presented. The CERN's project was called Energy Amplifier [1] and the second project Accelerator Transmutation of Waste (ATW) [2] was planned at the Los Alamos National Laboratory. Nowadays, ADS research is still realized in whole world. For example, Europe has one main project which is under development. The MYRRHA project [3] was planned since 1997 in Belgium.

One of the most important part of the ADS is the spallation target which generates neutrons by interactions of proton beam with the target. Material of the target is selected as heavy metals because the number of neutron produced by interaction with one proton is in the range of 20-30 [4]. The idea to irradiate light material mixed with heavy material was experimentally performed in Japan, where a multitarget made from lead and beryllium was irradiated by 100 MeV protons [5]. The similar idea is planned at the Joint Institute for Nuclear Research (JINR). Here, two elongated targets from lead and carbon were irradiated by high energy proton beam. The detection of secondary neutrons was performed by threshold activation detectors which were placed at the axis of the targets.

2 Experimental part

The experimental irradiations were carried out at the Dzhelepov Laboratory of the Nuclear Problems, JINR, Dubna, Russian Federation, at the synchrocyclotron Phasotron accelerator. The experiments were arranged with carbon target on 25. 05. 2018 and with lead spallation target on 08. 06. 2018. The cobalt samples were used for neutron and proton detection. The experimental part describes the set-ups and provides basic information about irradiations.

2.1 Carbon target

The first target is composed of carbon discs which were 190 mm in diameter and the width of one disc was 100 mm. The total number of discs was 10 and two discs formed one section. The neighboring sections were separated by 10 mm air gap. The length of the set-up was 1 040 mm. The side view of the target is shown in Fig. 1. The figure illustrates direction of the proton beam as well.

2.2 Lead target

The next irradiation experiment was arranged with the lead target which was made of discs 190 mm in diameter and

*e-mail: zemanm@feec.vutbr.cz

the thickness 52 mm. The total number of discs was 20 and the length of the set-up was 1 080 mm. The target was divided in 5 sections. Four sections were similar with the 104 mm thickness (two discs in one section) and the fifth section was composed of 12 discs with the length of 624 mm. The 10 mm air gaps were chosen for detection of proton beam in the central part of the target. The stand was placed at concrete blocks and wooden desk during the experiment.

2.3 Experimental irradiations

The targets were irradiated by 660 MeV proton beam produced by Phasotron accelerator. The samples of ^{59}Co were irradiated in the secondary neutron field generated inside of the lead and carbon targets. The samples were situated at the surface of the set-ups. The dimension of the "Z" axis is shown in Fig.1, the dimension of "X" axis was -38 mm and parameter of "Y" axis was 88 mm. The parameters X;Y;Z axis in 0;0;0 was related to center of the first cylinder. Location of ^{59}Co samples were the same for both experiments.

Samples of cobalt in the carbon experiment were 1 mm in thickness, squared shapes with 20x20 mm^2 and mass approximately 3.5 g. The samples at the lead experiment were of the same thickness but had the dimensions 10x10 mm^2 and mass approximately 0.85 g for first 6 samples and the rest 4 samples were of 10x15 mm^2 squared shape with approximate weight 1.35 g.

The carbon target was irradiated for 6 hours and 5 minutes and the number of protons was 2.35(18)E15. The proton integral was determined 2.32(19)E15 during the 6 hour irradiation of the lead set-up. The proton integral was determined by three aluminum and copper activation monitors.

3 Data analysis

The measured spectra of ^{59}Co samples were analyzed using the gamma-ray spectroscopy software DEIMOS32 [6]. Another part was focused on the calculation of the experimental reaction rates of radionuclides in the ^{59}Co samples. The reaction rate was defined as the number of produced residual nuclei per one atom in the sample and one incident proton. The reaction rates were analyzed with an in-house software [7].

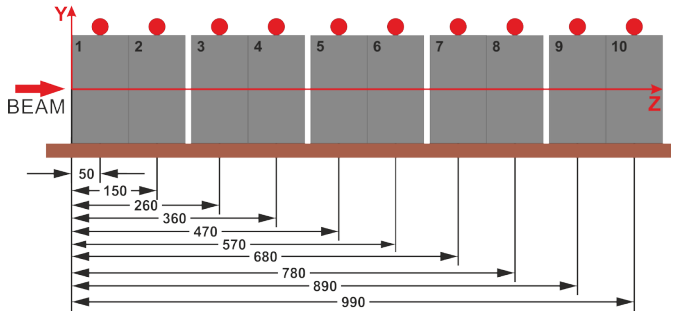

Figure 1. Scheme of the Carbon target with locations of the experimental samples.

The final form of the equation to determine the experimental reaction rate is:

$$Rr = \frac{S(E_\gamma)C_{abs}B_a}{I_\gamma \varepsilon(E_\gamma)} \cdot \frac{t_{real}}{t_{live}} \cdot \frac{1}{N_A N_P} \cdot \frac{e^{(\lambda t_0)}}{1 - e^{(-\lambda t_{real})}} \cdot \frac{\lambda t_{irr}}{1 - e^{(-\lambda t_{irr})}} \cdot \frac{1}{C_{coisum}}, \quad (1)$$

where $S(E_\gamma)$ is the peak area, C_{abs}(E$_\gamma$) is the self-absorption correction, B_a is the beam intensity correction, I_γ is the gamma-line intensity per decay, $\varepsilon(E_\gamma)$ is the full-energy peak efficiency, t_{real} is the real measurement time, t_{live} is the live time of the measurement, N_A is the number of atoms in the sample, N_P is the number of incident particles during irradiation, t_0 is the time between the end of irradiation and start of the measurement, λ is the decay constant, t_{irr} is the time of irradiation, and C_{coisum} is the correction for true coincidence summing [8].

4 Experimental results and Discussion

4.1 Results from carbon experiment

The results of gamma-ray spectroscopy measurements provided 7 reactions with various threshold energies generated by interaction of ^{59}Co with neutrons (up to 48.5 MeV) or protons (up to 24 MeV).

The measured data are shown in Figures 2, 3, and 4. The upper part of graphs present information on reaction rates of each reaction from samples at different positions at longitudinal distance. All reactions were detected at whole longitudinal distance of the set-up and the maximal production of reaction rates was at the sample situated at 260 mm from the beginning of the target. This is valid except for the $^{59}Co(n,\gamma)^{60}Co$ reaction because here the maximum is at 360 mm. The results of reaction rates were compared with the value calculated at position 260 mm from the front side of the target. Results of calculations are presented in lower part of the above mentioned graphs. Following reaction rates of radionuclides have similar shape of curves, except for the $^{59}Co(n,\gamma)^{60}Co$ reaction which was not steep.

4.2 Results from lead experiment

Reaction rates of radionuclides produced in ^{59}Co samples, which were induced by neutron field generated in elongated target, are presented in Figures 5, 6, and 7.

The maximal production of secondary neutrons was at the position of 150 mm from the front side of the lead target and protons were absorbed between 360 mm and 470 mm from the beginning of the set-up. High energy neutrons, with the energy higher than 48.5 MeV (threshold of $^{59}Co(n,5n)^{55}Co$ reaction), were not detected from the distance of 680 mm from the beginning because the number of high energy neutrons in the area was very low. Also, 34.3 MeV neutrons causing $^{59}Co(n,4n)^{56}Co$ reaction are not detected at distance 990 mm from the beginning. The ratios of reaction rates shown in lower part of graphs below were from 0.0014 for $^{59}Co(n,2n)^{58}Co$ at 990 mm from the beginning up to 1.21 for $^{59}Co(p,3n)^{57}Ni$ reaction.

Table 1. Ratios of produced reaction rates of $^{59}Co(n,\gamma)^{60}Co$, $^{59}Co(n,p)^{59}Fe$, $^{59}Co(n,2n)^{58}Co$, $^{59}Co(n,3n)^{57}Co$, $^{59}Co(n,4n)^{56}Co$, $^{59}Co(n,5n)^{55}Co$, and $^{59}Co(p,3n)^{57}Ni$ evaluated from carbon and lead experiments.

Product	^{60}Co	^{59}Fe	^{58}Co	^{57}Co	^{56}Co	^{55}Co	^{57}Ni
Distance	Ratios of Carbon/Lead experiments						
(mm)	(-)						
50	0.066(9)	0.092(12)	0.185(31)	0.247(32)	0.354(45)	0.54(7)	1.55(34)
150	0.09(1)	0.168(22)	0.397(75)	0.513(67)	0.829(108)	1.24(17)	2.81(55)
260	0.103(14)	0.303(39)	0.704(12)	0.885(115)	1.45(18)	2.11(28)	5.081(873)
360	0.133(18)	0.729(94)	1.595(31)	1.98(26)	3.14(41)	4.81(65)	15.1(31)
470	0.175(25)	2.01(26)	4.51(92)	5.05(69)	8.2(11)	11.3(17)	-
570	0.237(32)	4.81(65)	8.19(128)	12.3(17)	18.3(25)	25.3(46)	-
680	0.302(41)	10.0(14)	17.8(28)	30(4)	44(7)	-	-
780	0.337(45)	16.7(26)	29.2(50)	48.5(67)	34(10)	-	-
890	0.371(52)	19.9(49)	45(8)	77(11)	121(50)	-	-
990	0.345(55)	18.84(737)	54.4(101)	107(17)	-	-	-

4.3 Comparison of reaction rates following at carbon and lead experiments

The last part of experimental work compared the results from lead and carbon experiments. All the following ratios are shown in Table 1. The results of the (n,γ) reaction were lower in experiment with carbon target in the whole set-up. Other reaction rates for the following reactions were higher in the experiment with the lead target and a "breaking point", position where the reaction rates from experiment with lead target were higher than results at carbon target, changed at various longitudinal distances. The reaction with higher threshold energy has been close to the beginning of the set-ups. The results of $^{59}Co(p,3n)^{57}Ni$ reaction were higher at 50 mm from the carbon target than lead experiment.

5 Conclusion

Two irradiation experiments were performed with carbon and lead elongated targets by 660 MeV proton beam and the threshold detectors of cobalt were placed at the surface of the set-ups. Produced radionuclides were analyzed and determined by gamma-ray spectroscopy. The products with threshold energy 34.5 MeV were calculated to the position 890 mm from the beginning and products with threshold 48.5 MeV were calculated only to 570 mm from the beginning of lead target. The $^{59}Co(p,n3)^{57}Ni$ reaction was measured at all samples of carbon target and to 360 mm from the beginning of lead target. The proton reaction can be produced by scattering of proton beam or production of protons from other reactions. The comparison of carbon and lead experiments showed that both materials produced different neutron and proton fields because of different results of reaction rates of analyzed radionuclides. Future experiments can be focused on multi-material lead-carbon target.

Acknowledgments

This research work has been carried out within the ADAR project (Accelerator Driven Advanced Reactor). Authors gratefully acknowledge financial support from the Ministry of Education, Youth and Sports of the Czech Republic under INTER-ACTION research programme (project No. LTAUSA18198). Authors gratefully acknowledge financial support from the Ministry of Education, Youth

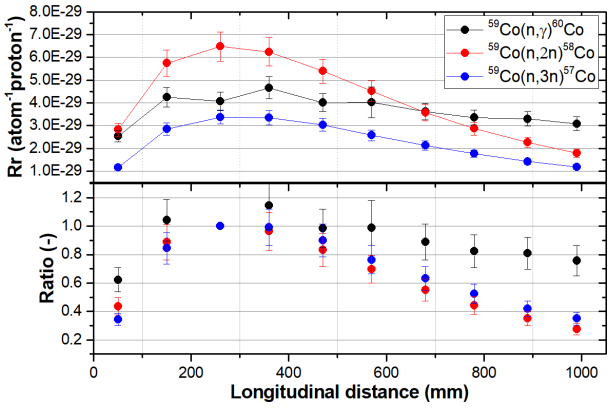

Figure 2. Determination and comparison of $^{59}Co(n,\gamma)^{60}Co$, $^{59}Co(n,2n)^{58}Co$, and $^{59}Co(n,3n)^{57}Co$ reaction rates at carbon experiment.

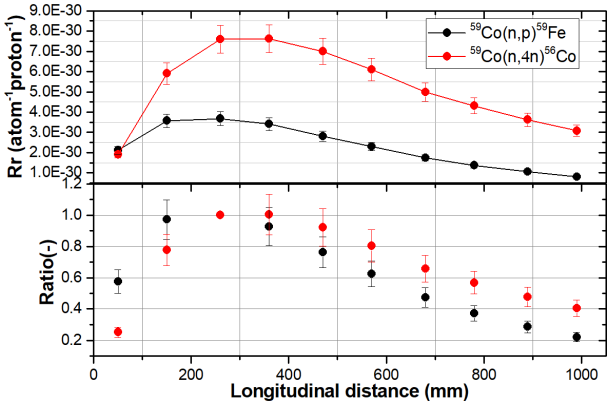

Figure 3. Determination and comparison of $^{59}Co(n,p)^{59}Fe$, and $^{59}Co(n,4n)^{56}Co$ reaction rates at carbon experiment.

and Sports of the Czech Republic under Brno University of Technology specific research programme (project No. FEKT-S-17-4784 "New Technologies for sustainable power engineering") and under international research cooperative programme of JINR Dubna and the Czech Republic (projects of joint 3+3 committee No. 12/159/2018 "Study of neutron flux in spallation targets"). Author thanks to Mr. Radek Vespalec for innovation of software package for reaction rate calculations.

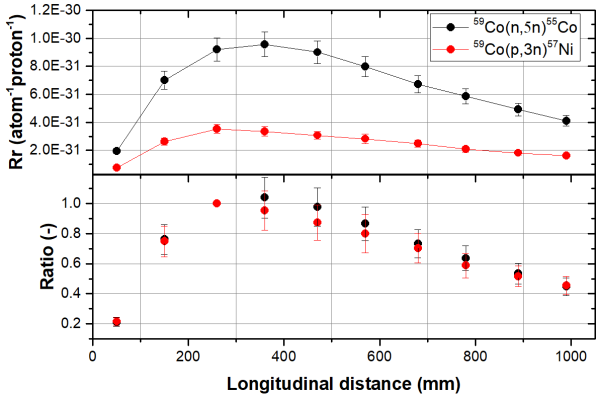

Figure 4. Determination and comparison of $^{59}Co(n,5n)^{55}Co$, and $^{59}Co(p,n3)^{57}Ni$ reaction rates at carbon experiment.

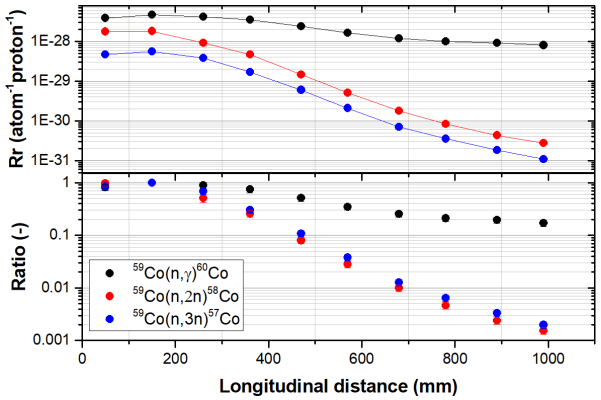

Figure 5. Determination and comparison of $^{59}Co(n,\gamma)^{60}Co$, $^{59}Co(n,2n)^{58}Co$, and $^{59}Co(n,3n)^{57}Co$ reaction rates at lead experiment.

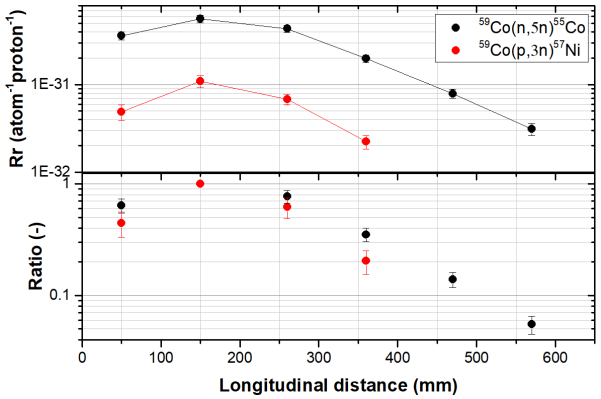

Figure 7. Determination and comparison of $^{59}Co(n,5n)^{55}Co$, and $^{59}Co(p,n3)^{57}Ni$ reaction rates at lead experiment.

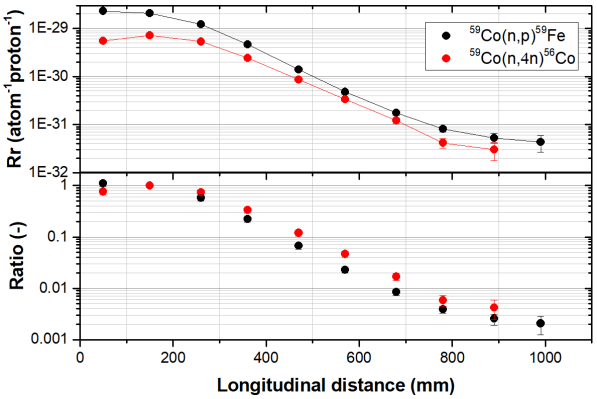

Figure 6. Determination and comparison of $^{59}Co(n,p)^{59}Fe$, and $^{59}Co(n,4n)^{56}Co$ reaction rates at lead experiment.

References

[1] C. Rubbia, J.A. Rubio, S. Buono, Tech. rep., International Atomic Energy Agency (IAEA) (1997), iAEA-TECDOC–985

[2] C. Bowman, E. Arthur, P. Lisowski, G. Lawrence, R. Jensen, J. Anderson, B. Blind, M. Cappiello, J. Davidson, T. England et al., Nuclear Instruments and Methods in Physics Research Section A: Accelerators, Spectrometers, Detectors and Associated Equipment **320**, 336 (1992)

[3] H.A. Abderrahim, P. Baeten, D.D. Bruyn, R. Fernandez, Energy Conversion and Management **63**, 4 (2012), 10th International Conference on Sustainable Energy Technologies (SET 2011)

[4] W. Chou, Tech. rep., United States (Feb 2003), fERMILAB-Conf–03/012, `https://www.osti.gov/servlets/purl/807534-Nn4e0c/native/`

[5] Y. Takahashi, T. Azuma, T. Nishio, T. Yagi, C.H. Pyeon, T. Misawa, Annals of Nuclear Energy **54**, 162 (2013)

[6] J. Frána, Journal of Radioanalytical and Nuclear Chemistry **257**, 583 (2003)

[7] I. Adam, J. Mrazek, J. Frána, A.R. Balabekyan, V.S. Pronskikh, V.G. Kalinnikov, A.N. Priemyshev, Measurement Techniques **44**, 93 (2001)

[8] INTERNATIONAL ATOMIC ENERGY AGENCY, *Specialised Software Utilities for Gamma Ray Spectrometry* (2002), iAEA-TECDOC-1275, `http://www-pub.iaea.org/books/IAEABooks/6359/Specialised-Software-Utilities-for-Gamma-Ray-Spectrometry`